NASA Contractor Report 4279

A 4-Node Assumed-Stress Hybrid Shell Element With Rotational Degrees of Freedom

Mohammad A. Aminpour
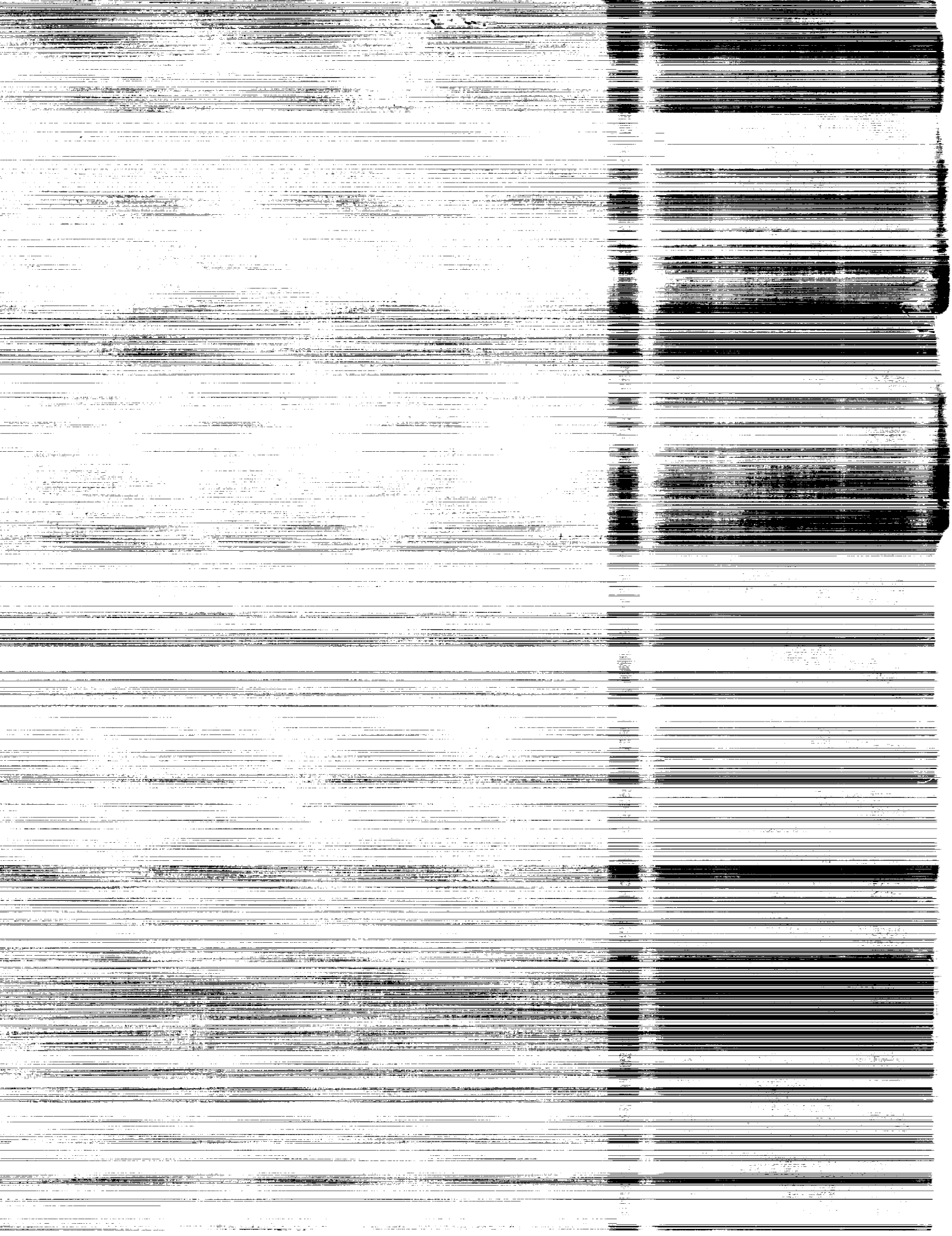
A 4-Node Assumed-Stress Hybrid Shell Element With Rotational Degrees of Freedom

Mohammad A. Aminpour
Analytical Services & Materials, Inc.
Hampton, Virginia

NASA

National Aeronautics and
Space Administration

Office of Management

Scientific and Technical
Information Division

1990

A 4-Node Assumed-Stress Hybrid Shell Element with Rotational Degrees of Freedom

M. A. AMINPOUR

Analytical Services & Materials, Inc.

Hampton, VA 23666

Abstract

An assumed-stress hybrid/mixed 4-node quadrilateral shell element is introduced that alleviates most of the deficiencies associated with such elements. The formulation of the element is based on the assumed-stress hybrid/mixed method using the Hellinger-Reissner variational principle. The membrane part of the element has 12 degrees of freedom including rotational or "drilling" degrees of freedom at the nodes. The bending part of the element also has 12 degrees of freedom. The bending part of the element uses the Reissner-Mindlin plate theory which takes into account the transverse shear contributions. The element formulation is derived from an 8-node isoparametric element. This process is accomplished by assuming quadratic variations for both in-plane and out-of-plane displacement fields and linear variations for both in-plane and out-of-plane rotation fields along the edges of the element. In addition, the degrees of freedom at midside nodes are approximated in terms of the degrees of freedom at corner nodes. During this process the rotational degrees of freedom at the corner nodes enter into the formulation of the element. The stress field is expressed in the element natural-coordinate system such that the element remains invariant with respect to node numbering. The membrane part of the element is based on a 9-parameter stress field, while the bending part of the element is based on a 13-parameter stress field. The element passes the patch test, is nearly insensitive to mesh distortion, does not "lock", possesses the desirable invariance properties, has no spurious modes, and for the majority of test cases used in this paper produces more accurate results than the other elements employed herein for comparison.

Introduction

The finite element method is a powerful technique that is used to solve a variety of very complicated problems in different fields of engineering and science. In the field of structural mechanics, the finite element method is the most widely used method for obtaining solutions to structural analysis problems. The finite element modeling of general aerospace shell structures usually requires the use of distorted meshes. Additional complexities arise if the original finite element discretization is further refined through an adaptive refinement procedures. Most of the 4-node shell elements developed in the past do not produce reliable results for distorted meshes. The element developers are usually aware of the limitations and pitfalls of the elements. The users, on the other hand, may not be aware of all these limitations and make invalid uses of the these elements. It is desirable to develop simple 3-node and 4-node shell elements that are free from these limitations and pitfalls, such as spurious zero-energy modes, locking, sensitivity to mesh distortion, invariant properties,

and most importantly produce accurate and reliable results. The elements that have been developed to date lack one or more of these characteristics. The standard 3-node and 4-node isoparametric elements are generally too stiff for most practical problems, and a "blizzard" of these elements must be used to model even simple shell structures in order to obtain accurate and reliable results. In order to remedy the situation, researchers have developed many non-standard elements which have their own merits and shortcomings. Some of these elements do not pass the patch test—a requirement for convergence to the correct solution. Some other elements have spurious mechanisms (zero-energy deformational modes) such as the hour-glass mode, while some others do not possess the desirable invariance properties with respect to node numbering. Furthermore, most elements are sensitive to geometry or mesh distortion.

One way to remedy the deficiencies of the *membrane* elements is to include the nodal rotational or "drilling" degrees of freedom in the element formulation. In early attempts, these rotational degrees of freedom were used in cubic displacement functions. However, Irons and Ahmad demonstrated that this concept had serious deficiencies[1]. The elements formed in such a manner force the shearing strain to be zero at the nodes and do not pass the patch test, which could produce serious error in some structural analysis problems. Recently several researchers have used these rotational degrees of freedom in quadratic displacement functions with more success[2-5]. This latter method is constructed in the following way. First, the element is internally assumed to be an 8-node (4 corner nodes and 4 midside nodes) isoparametric element with 16 degrees of freedom and the stiffness matrix associated with this "internal" element is calculated. Then, this stiffness matrix is condensed to that of a 4-node element with 12 degrees of freedom by associating the displacement degrees of freedom at the midside nodes with the displacement and rotational degrees of freedom at the corner nodes. MacNeal[4] has used this approach to develop 4-node displacement-based *membrane* elements with selective reduced-order integration. Yunus et al.[5] have also used this method to develop assumed-stress hybrid/mixed *membrane* elements.

In this paper, this method is extended to the *plate* problem as well as the *membrane* problem to develop a 4-node assumed-stress hybrid/mixed quadrilateral *shell* element with 24 degrees of freedom. The formulation is based on the Hellinger-Reissner variational principle. The element formulation is derived from an 8-node isoparametric shell element with 40 degrees of freedom by eliminating the degrees of freedom at the midside nodes at the expense of adding the rotational degrees of freedom to the corner nodes. This process is accomplished by assuming quadratic variations for both in-plane and out-of-plane boundary displacements and linear variations for both in-plane and out-of-plane boundary rotations along the edges of the element and evaluating these functions at the midside locations. These midside values are then used to condense the stiffness matrix of the 8-node element to that of the 4-node element. As a result, the rotational degrees of freedom at the corner nodes enter into the formulation.

The membrane part of the element has 12 degrees of freedom, three of which account for the rigid body modes. Therefore, a minimum of 9 independent stress parameters are needed to avoid rank deficiency for the membrane part. The bending part of the element

also has 12 degrees of freedom, three of which account for the rigid body modes. Therefore, a minimum of 9 independent stress parameters are also needed to avoid rank deficiency for the bending part. The membrane stress field is represented with 9 independent parameters. The bending stress field, on the other hand, is represented with 13 independent parameters which was derived in references [6-8] through an asymptotic power-series expansion of stresses in the thickness direction. This 13 parameter selection of stresses for the bending part is less sensitive to geometry or mesh distortion than a 9 parameter selection obtained from a degenerate solid model[9].

Evolution of Hybrid Method

The classical assumed-stress hybrid formulation of Pian[10] is based on the principle of minimum complementary energy. The displacements are described only along the element boundary, and an equilibrating stress field is described over the domain of the element. It was later recognized that the same method may be derived from the Hellinger-Reissner principle[11-13]. However, in the Hellinger-Reissner principle the stress field is not required to satisfy the equilibrium equations a priori, while the displacement field must be described over the domain of the element and not just along the boundaries. The stress field would then satisfy the equilibrium equations only in a variational sense. Therefore, the stress field may be described in the natural-coordinate system of the element which would make the element less sensitive to mesh distortion, and a proper selection of the stress field would make the element invariant with respect to node numbering. For example, if the node numbering is changed from 1-2-3-4 to 2-3-4-1, then the natural coordinate of the element would rotate by 90^0. Therefore, a selection of stresses that is invariant under a 90^0 rotation would make the element invariant. Because of these desirable attributes, researchers have developed assumed-stress hybrid/mixed elements using the Hellinger-Reissner principle.

In this study, the Hellinger-Reissner principle is used to develop a 4-node shell element, which includes the rotational degrees of freedom in the membrane part of the element formulation. The details of the assumed-stress hybrid/mixed formulation using the Hellinger-Reissner principle has been extensively discussed in the literature (e.g., see references [11-13]), and only a brief outline is given herein for completeness. The variational functional is given as

$$\Pi = -\frac{1}{2} \int_V \sigma^T \mathbf{D} \sigma dV + \int_V \sigma^T \mathcal{L}[\mathbf{u}] dV - \int_{S_t} \mathbf{u}^T \mathbf{t_0} dS \qquad (1)$$

where $\mathbf{D}$ is the compliance matrix of the material, σ is the stress array, $\mathbf{u}$ is the displacement array, $\mathbf{t_0}$ is the prescribed traction array, matrix $\mathcal{L}$ is a differential operator which produces a strain field when operated on the displacement field, V is the domain of the element, and S_t is the part of the boundary where $\mathbf{t_0}$ is specified. The assumed-stress hybrid/mixed formulation is based on assuming a stress field in the interior of the element as

$$\sigma = \mathbf{P}\beta \qquad (2)$$

and assuming the displacement field as

$$\mathbf{u} = \mathbf{N}\mathbf{q} \qquad (3)$$

3

where the matrices **P** and **N** consist of the appropriate interpolating functions for stresses and displacements, respectively, and the vectors β and **q** are the unknown stress parameters and nodal displacements and rotations, respectively.

The expressions for stresses in equation (2) and displacements in equation (3) are substituted into the functional Π of equation (1) and the variation of the functional with respect to the element internal unknowns β are set to zero. This stationary condition gives

$$\beta = \mathbf{H}^{-1}\mathbf{T}\mathbf{q} \tag{4}$$

where

$$\mathbf{H} = \int_V \mathbf{P}^T \mathbf{D}\mathbf{P} dV \tag{5}$$

$$\mathbf{T} = \int_V \mathbf{P}^T \mathcal{L}[\mathbf{N}] dV \tag{6}$$

The substitution of the expression for β in equation (4) into the functional Π of equation (1) and a subsequent variation of the functional with respect to the global unknowns **q** yields

$$\mathbf{K}\mathbf{q} = \mathbf{F} \tag{7}$$

where the stiffness matrix **K** is given by

$$\mathbf{K} = \mathbf{T}^T \mathbf{H}^{-1} \mathbf{T} \tag{8}$$

and the generalized force vector **F** by

$$\mathbf{F} = \int_{S_t} \mathbf{N}^T \mathbf{t}_0 dS \tag{9}$$

Element Formulation

Midside Displacement Approximation

As discussed earlier, the stiffness matrix for the present 4-node element is obtained from the stiffness matrix associated with the "internal" 8-node element shown in Figure 1. This process is accomplished by associating the degrees of freedom at midside nodes with the degrees of freedom at corner nodes by expressing the displacement components along each edge of the element as quadratic functions in terms of the nodal displacements and rotations as follows. If a typical edge of a quadrilateral is considered to be a 2-node beam (see Fig. 1, edge 1) with constant shear deformations then a displacement component perpendicular to the beam axis, for example the v' component, may be described as a quadratic function as

$$v' = a_0 + a_1\xi + a_2\xi^2 \tag{10}$$

where, ξ is a non-dimensional coordinate in the direction of the axis of the beam such that node 1 of the beam is at $\xi = -1$ and node 2 of the beam is at $\xi = +1$.

The rotation about the z axis, θ_z, is given by

$$\theta_z = \frac{\partial v'}{\partial x'} - \gamma' \tag{11}$$

where γ' is the constant shear deformation of the beam in the x-y plane. The four unknowns a_0, a_1, a_2 in equation (10), and γ' in equation (11) may be solved for in terms of the two nodal displacements v'_1 and v'_2 and the two nodal rotations θ_{z1} and θ_{z2}. The displacement component v' is given by

$$v' = \frac{1}{2}(1 - \xi)v'_1 + \frac{1}{2}(1 + \xi)v'_2 - \frac{l}{8}(1 - \xi^2)(\theta_{z2} - \theta_{z1}) \tag{12}$$

where l is the length of the beam. The normal or "drilling" rotation is given by

$$\theta_z = \frac{1}{2}(1 - \xi)\theta_{z1} + \frac{1}{2}(1 + \xi)\theta_{z2} \tag{13}$$

and the shearing strain by

$$\gamma' = \frac{1}{l}(v'_2 - v'_1) - \frac{1}{2}(\theta_{z2} + \theta_{z1}) \tag{14}$$

The displacement parallel to the beam axis is described as a linear function in terms of the two nodal displacements as

$$u' = \frac{1}{2}(1 - \xi)u'_1 + \frac{1}{2}(1 + \xi)u'_2 \tag{15}$$

These concepts may be readily extended to triangular and quadrilateral elements. Therefore, the in-plane displacement and rotation fields on a typical edge of a quadrilateral element (e.g., edge 1 of Fig. 1) expressed in the element reference x-y coordinate system may be described as

$$u = \frac{1}{2}(1 - \xi)u_1 + \frac{1}{2}(1 + \xi)u_2 + \frac{\Delta y_1}{8}(1 - \xi^2)(\theta_{z2} - \theta_{z1})$$

$$v = \frac{1}{2}(1 - \xi)v_1 + \frac{1}{2}(1 + \xi)v_2 - \frac{\Delta x_1}{8}(1 - \xi^2)(\theta_{z2} - \theta_{z1}) \tag{16}$$

$$\theta_z = \frac{1}{2}(1 - \xi)\theta_{z1} + \frac{1}{2}(1 + \xi)\theta_{z2}$$

where, Δx_1 and Δy_1 are the Δx and Δy of edge 1 with respect to the reference local element x-y coordinate system (e.g., $\Delta x_1 = x_2 - x_1$). Note that only the displacement functions described in equations (16) enter into the membrane formulation. It should be mentioned here that the true nodal rotations are given by $\frac{1}{2}(\frac{\partial v}{\partial x} - \frac{\partial u}{\partial y})$ evaluated at the nodes. Hence, the terms θ_{zi} are not true nodal rotations, and they may be referred to as "rotational connectors"[2].

5

In references [2-5], the above displacement functions were used for construction of membrane elements. However, this same procedure may also be used for development of a bending element. Again, quadratic functions are used to describe the out-of-plane displacement component w and linear functions are used to described the out-of-plane rotations θ_x and θ_y along each edge of the element. The final result for the out-of-plane displacement and rotation fields on edge 1 of Figure 1 is

$$w = \frac{1}{2}(1-\xi)w_1 + \frac{1}{2}(1+\xi)w_2 - \frac{\Delta y_1}{8}(1-\xi^2)(\theta_{x2} - \theta_{x1}) + \frac{\Delta x_1}{8}(1-\xi^2)(\theta_{y2} - \theta_{y1})$$

$$\theta_x = \frac{1}{2}(1-\xi)\theta_{x1} + \frac{1}{2}(1+\xi)\theta_{x2} \tag{17}$$

$$\theta_y = \frac{1}{2}(1-\xi)\theta_{y1} + \frac{1}{2}(1+\xi)\theta_{y2}$$

Equations (16) and (17) indicate that both the membrane part and the bending part of the element are formulated in the same manner. All three displacement components are quadratic functions, while all three rotations are linear functions. This conformity in the order of the approximating polynomials for all displacement components and all rotation components is very desirable in the analysis of shell problems.

The basic concept of the element is similar to that of Cook's proposed 4-node membrane element[3]. However, this concept is extended in this paper to the bending problem in order to construct a 4-node flat shell element. Internally the element is an 8-node isoparametric quadrilateral element. Externally, the midside degrees of freedom of the 8-node element are approximated by the above displacement and rotation functions, so that the midside degrees of freedom are eliminated at the expense of adding drilling degrees of freedom to the 4-node element. For example, on edge 1 of Figure 1, the midside degrees of freedom are given by evaluating the functions in equations (16) and (17) at $\xi = 0$. This gives

$$u_5 = \frac{1}{2}(u_1 + u_2) + \frac{\Delta y_1}{8}(\theta_{z2} - \theta_{z1})$$

$$v_5 = \frac{1}{2}(v_1 + v_2) - \frac{\Delta x_1}{8}(\theta_{z2} - \theta_{z1})$$

$$w_5 = \frac{1}{2}(w_1 + w_2) - \frac{\Delta y_1}{8}(\theta_{x2} - \theta_{x1}) + \frac{\Delta x_1}{8}(\theta_{y2} - \theta_{y1}) \tag{18}$$

$$\theta_{x5} = \frac{1}{2}(\theta_{x1} + \theta_{x2})$$

$$\theta_{y5} = \frac{1}{2}(\theta_{y1} + \theta_{y2})$$

The description for other midside nodes is readily obtained. It is not necessary to evaluate the function θ_z in equations (16) at $\xi = 0$ since the normal rotation θ_z does not enter into the membrane formulation. It is observed that the extra nodal degrees of freedom are

associated with the membrane part of the element only. The bending part of the problem does not add any extra degrees of freedom to the element.

Equations (16), when extended to all four sides of the element, indicate that the membrane part of the element has 12 degrees of freedom. Two of these are the in-plane translational rigid body motions and one is the in-plane rotational rigid body motion. Of the nine remaining degrees of freedom, three represent the constant strain states, five represent higher-order strain states, and the final degree of freedom represents a special type of zero-energy "spurious" mode. This zero-energy mode is associated with a state of zero nodal displacements and equal nodal rotations. This state renders the u and v displacement components in equations (16) zero on all four sides of the quadrilateral, while all four corner nodes of the quadrilateral are rotated about its normal by equal amounts Θ_z. This mode is shown in Figure 2 using cubic interpolation for displacements and may be called a "zero displacement" mode[2]. It occurs because the quadratic displacement functions are based on the differences of the nodal rotations and not the nodal rotations themselves. One of these differences is dependent on the other three. Therefore, the membrane part of the element has, in fact, only 11 independent displacement modes but is expressed in terms of 12 degrees of freedom. Hence, one of the normal rotational degrees of freedom is extraneous and must be eliminated. This zero-energy mode is of a special type and is different from other spurious mechanisms such as the hour-glass mode. In reference [4], this zero-energy mode is removed by artificially adding a small energy penalty to the stiffness matrix to make the stiffness matrix non-singular. Although, this could be accomplished with little effort, prescribing the value of normal rotation for at least one node in the entire finite element model of the structure will eliminate this extraneous degree of freedom.

Equations (17) indicate that the bending part of the element also has 12 degrees of freedom. One of these is the out-of-plane translational rigid body motion and two of these are the out-of-plane rotational rigid body motions. Of the nine remaining degrees of freedom, three represent the constant curvature states, two represent the constant transverse shear strain states, and the other four represent higher-order strain states. No zero-energy modes are associated with the bending part of the element. Note that although the displacement function w described in equations (17) is also in terms of the differences of the nodal rotations and not the rotations themselves, each one of the nodal rotations are accounted for by the functions θ_x and θ_y in equations (17). This is not the case for the membrane part because the rotation function θ_z in equations (16) does not enter into the membrane formulation, while both rotation functions θ_x and θ_y in equations (17) enter into the bending formulation.

Stress Field Description
The stress field should be selected in such a manner that no spurious zero-energy mode is produced. A spurious zero-energy mode is produced when the product of a selected stress term and the strains that are derived from the displacement functions produces zero strain energy under a particular, but not trivial, deformational displacement field. In order to avoid spurious zero-energy modes, each independent stress term must suppress one independent deformation mode. The problem of spurious zero-energy modes generally occurs for regular geometries such as rectangular planar elements and brick solid elements

and it disappears for irregular geometries[14].

As discussed previously, the membrane part of the element has 12 degrees of freedom—three of which are due to the in-plane rigid body motions. Therefore, a stress field with a minimum of 9 independent parameters is needed to describe the membrane stress (resultant) field. The following stress (resultant) field is first considered for the membrane part

$$N_\xi = \beta_1 + \beta_4\eta + \beta_6\xi + \beta_8\xi\eta$$

$$N_\eta = \beta_2 + \beta_5\xi + \beta_7\eta + \beta_9\xi\eta$$

$$N_{\xi\eta} = \beta_3 - \beta_6\eta - \beta_7\xi - \frac{1}{2}\beta_8\eta^2 - \frac{1}{2}\beta_9\xi^2$$

$$(19)$$

This stress (resultant) field is obtained by integrating, through the thickness, the components of the contravariant stress tensor expressed in the natural coordinates. These components must be transformed to the physical stress components in the element reference coordinates by contravariant tensor transformation laws. However, the components of the transformation are evaluated at the origin of the natural coordinates in order to retain the constant terms in the stress field description[11-13]. When the stress (resultant) field in equations (19) is specialized to the rectangular coordinate system, the stress resultants of the stress field assumed by Robinson[15,16] for his 8-node and 4-node membrane elements are obtained. In the above stress (resultant) field, the first five terms represent the stress field that was used in Pian's 4-node assumed-stress hybrid membrane element which had no rotational degrees of freedom[11-13]. The remaining terms are present to suppress the rotational degrees of freedom present in this formulation. However, experimentations with a single rectangular element revealed that the stress (resultant) field in equations (19) produces one spurious zero-energy mode. It should be mentioned here that Robinson's suggested stress field worked for his formulation which was based on a cubic displacement field. Therefore, it is proposed herein to use the following 9-term stress field for the membrane part

$$N_\xi = \beta_1 + \beta_4\eta + \beta_6\xi + \beta_8\eta^2$$

$$N_\eta = \beta_2 + \beta_5\xi + \beta_7\eta + \beta_9\xi^2$$

$$N_{\xi\eta} = \beta_3 - \beta_6\eta - \beta_7\xi$$

$$(20)$$

This stress field produces no spurious zero-energy mode for the assumed displacement field described in equations (16) for the membrane part. When the elements are rectangular in shape this selection of stress field satisfies the equations of equilibrium a priori. In reference [5], a different 9-term stress field was selected which assumes linear variation for all stress components which satisfies equilibrium in a variational sense for all element geometries including rectangular-shaped elements.

The bending part of the element has 12 degrees of freedom—three of which are due to the out-of-plane rigid body motions. Therefore, a stress field with a minimum of 9 independent parameters is needed to describe the stress field. The following stress (resultant) field is

8

chosen for the bending part

$$M_\xi = \bar{\beta}_1 + \bar{\beta}_4\eta + \bar{\beta}_6\xi + \bar{\beta}_8\xi\eta$$

$$M_\eta = \bar{\beta}_2 + \bar{\beta}_5\xi + \bar{\beta}_7\eta + \bar{\beta}_9\xi\eta \tag{21}$$

$$M_{\xi\eta} = \bar{\beta}_3 + \bar{\beta}_{10}\xi + \bar{\beta}_{11}\eta + \frac{1}{2}\bar{\beta}_{12}\xi^2 + \frac{1}{2}\bar{\beta}_{13}\eta^2$$

The transverse shear forces are taken to be derived from the moments such that the equilibrium equations are satisfied for rectangular elements

$$Q_\xi = M_{\xi,\xi} + M_{\xi\eta,\eta}$$

$$Q_\eta = M_{\xi\eta,\xi} + M_{\eta,\eta} \tag{22}$$

which gives

$$Q_\xi = (\bar{\beta}_6 + \bar{\beta}_{11}) + (\bar{\beta}_8 + \bar{\beta}_{13})\eta$$

$$Q_\eta = (\bar{\beta}_7 + \bar{\beta}_{10}) + (\bar{\beta}_9 + \bar{\beta}_{12})\xi \tag{23}$$

Again, this stress (resultant) field is obtained by integrating, through the thickness, the components of the contravariant stress tensor expressed in the natural coordinates and must be transformed to the physical components in the element reference coordinates by contravariant tensor transformation laws. As for the membrane part, the components of the transformation are evaluated at the origin of the natural coordinates in order to retain the constant terms in the stress field description. This stress field selection for the bending part satisfies the equations of equilibrium for rectangular-shaped elements a priori. When the above bending stress resultant field is specialized to the rectangular coordinate system, one obtains the resultants of the stress field that was derived in references [6-8]. The derivation of the stress field in references [6-8] consists of expressing the stress components as power series in the plate thickness, substituting these stresses into the continuum equations of elasticity, and equating the coefficients of like powers of the plate thickness. As discussed earlier, this 13 parameter selection of stresses for bending is less sensitive to geometric distortion than a 9 parameter selection obtained from a degenerate solid model[9]. This selection of stresses produces no spurious zero-energy modes.

In this paper, the Reissner-Mindlin Plate theory is used for the bending part. The bending part is of class C^0 and takes into account the effects of transverse shear deformations by assuming constant transverse shear strains through the thickness of the plate. This means that the transverse shear stresses are also constant through the thickness of the plate. However, generally the transverse shear stresses are zero on the plate surfaces. Therefore, a parabolic variation of transverse shear stresses and strains through the plate thickness is more reasonable. To account for this discrepancy, a static correction factor of 5/6 is included in the transverse shear strain energy, see Reissner[17].

Other Element Matrices
Other element matrices needed to complete the element formulation may be derived in a similar fashion. The element force vector **F** in equation (9) may be derived in a manner

9

consistent with the stiffness matrix. The surface traction and pressure loads are assumed to vary bilinearly over the element surface and the force vector **F** of equation (9) is calculated for the "internal" 8-node element. This force vector is then condensed to that of the 4-node element using the approximations for the midside degrees of freedom described earlier. For line load calculations, on the other hand, it is not necessary to use the "internal" 8-node element. The force vector **F** corresponding to line loads may be calculated directly based on the 4-node element by assuming linear variation of line loads on the edges of the element and using the displacement and rotation shape functions derived earlier.

The mass and geometric stiffness matrices for the present element may also be derived from the "internal" 8-node element in the same manner as for the stiffness matrix.

Numerical Results

Assessment of the 4-node quadrilateral shell element developed in this paper is presented in this section. The element has been implemented in the CSM Testbed Software System[18] using the generic element processor template[19]. Selected test problems include the patch test, the straight cantilever beam, the curved cantilever beam, the twisted cantilever beam, the Cook's tapered and swept panel, the thick-walled cylinder, and the Scordelis-Lo roof problem. The assumed-stress hybrid/mixed flat shell quadrilateral element derived in this paper will be referred to as AQR8 (Assumed-stress Quadrilateral Reduced from an 8-node element) in the following discussion for convenience. The results for the present element are compared with the results using the QUAD4 element of the MSC/NASTRAN from reference [20], the Q4S element of reference [4], the AQ element of reference [5], and the ES1/EX47, ES5/E410, and ES4/EX43 elements of the NASA Langley CSM Testbed. A brief description of these elements is given in the appendix. The dimensions and properties for the test problems are chosen in consistent units.

Patch Test
As the first test of the accuracy of the element, the patch test problem suggested in reference [20] is solved. This patch test is shown in Figure 3. Elements of arbitrary shapes are patched together to form a rectangular exterior boundary which makes it easy to apply boundary conditions corresponding to constant membrane strains and constant bending curvatures. The applied displacement boundary conditions and the theoretical solutions are also shown in Figure 3. The ability of the element to reproduce constant states of strains is an essential requirement for achieving convergence to the correct solution as the finite element mesh is refined. This requirement is observed by considering an individual element within a mesh with a complicated stress field. As the mesh is refined, the stresses within the elements tend towards a uniform value. Therefore, the elements that cannot produce a state of constant strains should not be trusted to converge to the correct solution as the mesh is refined[1]. The present element (AQR8) passes both the membrane and the bending patch tests with no error. The recovered strains and stresses are both exact.

Straight Cantilever Beam
As a second test, the straight cantilever beam problem suggested in reference [20] is solved for the three discretizations (six elements) shown in Figure 4. The constant and linearly

10

varying strains and curvatures are evoked by applying loads at the free end of the beam to test the ability of the element to recover these states of deformations. The theoretical results for extension, in-plane shear, out-of-plane shear, and in-plane moment are simply calculated from the elementary beam theory including shear deformations. The theoretical result for the twist is .03406, according to Timoshenko and Goodier's Theory of Elasticity[21]. Reference [20] quotes the answer to be .03208. Analysis with three successively refined meshes converged to .03385 which is much closer to the theory of elasticity solution than to that of reference [20]. Therefore, the solution from the theory of elasticity is taken herein for normalization purposes. The normalized results are shown in Table 1. The results show that all elements perform well for the rectangular mesh. However, for the trapezoidal and parallelogram meshes which contain considerable distortions, only the Q4S element and the present element (AQR8) are adequate. For the present element, while the error for all meshes and loads is less than 3.5%, the parallelogram mesh with a twist end load exhibits an error of 15.9% which shows the sensitivity of the selected bending stress field to mesh distortion.

Curved Cantilever Beam

Next, the curved cantilever beam problem shown in Figure 5 is solved. The beam is formed by a 90^0 circular arc. In-plane and out-of-plane loads are applied at the free end to produce in-plane and out-of-plane deformations, respectively. The theoretical solutions are taken to be those quoted in reference [20]. The normalized results from the present element (AQR8) are tabulated in Table 2. Also shown in Table 2 are the results from other elements for comparison. In this problem the mesh is distorted only slightly and the results for all elements are good. However, it is seen that the AQR8 element performs better than the other elements in the table, particularly for the in-plane shear loading.

Twisted Cantilever Beam

The twisted cantilever beam problem is shown in Figure 6. The beam is twisted 90^0 over its length. There are 12 elements along the length of the beam. Therefore, each element has a 7.5^0 warp. The beam is subjected to in-plane or out-of-plane unit loads at its free end. Both the membrane and the bending contributions are significant for either type of load. The theoretical solutions are taken to be those quoted in reference [20]. The normalized results from the present element (AQR8) are tabulated in Table 3. Also shown in Table 3 are the results from other elements for comparison. In this problem the mesh is comprised of rectangular shaped elements and there is no in-plane mesh distortion. Therefore, this problem tests the sensitivity of the elements due to warp distortion. The results show that, although the AQR8 element exhibits good performance, the QUAD4 element performs even better for this problem.

Cook's Tapered and Swept Panel

The tapered and swept panel with one edge clamped and the other edge loaded by a distributed shear force is analyzed next (see Fig. 7). This problem was used by Cook and many other researchers to test the sensitivities of finite elements due to geometric distortions. The panel was analyzed by a coarse 2×2 mesh and a finer 4×4 mesh. The reference solution for the vertical displacement at point C is taken to be 23.90 quoted in reference [5] as the best known answer. The normalized results for the present element

(AQR8) along with the results for other elements are shown in Table 4. The mesh for this problem is distorted only slightly and all the elements produce reasonable results. The AQR8 element, however, yields results that are closest to the best known answers.

Thick-Walled Cylinder
The thick-walled cylinder problem is shown in Figure 8. This problem was suggested by reference [20] to test the performance of finite elements for nearly incompressible materials. Plane strain conditions and radial symmetry are assumed so that the only non-zero displacement component is in the radial direction. The theoretical solution for this problem is given in any standard text book on elasticity (e.g., see reference [21]) and is shown in Figure 8. The normalized results for the present element (AQR8) along with the results for other elements are shown in Table 5. The mesh in this problem is distorted only slightly and the main purpose is to test the behavior of the elements for nearly incompressible materials. It is observed that, while the performance of the hybrid elements (i.e., the ES4/EX43 and the AQR8 element) does not deteriorate as the Poisson ratio approaches 0.5, the other elements fail to retain their performance. This insensitivity to nearly incompressible materials is a trait of assumed-stress hybrid elements.

Scordelis-Lo Roof
Finally, the Scordelis-Lo roof shown in Figure 9 is analyzed. This structure is a singly curved shell problem in which both the membrane and the bending contributions to the deformation are significant. The result reported in most references is the vertical displacement at the midpoint of the free-edge. The theoretical value for this displacement is quoted in reference [22] to be 0.3086, but the reference value quoted in reference [20] is 0.3024 for normalization of results. The latter value is also used herein for normalization purposes. Because of symmetry, only one quadrant of the problem is modeled. The mesh on one quadrant is chosen to be N×N for N=2,4,6,8,10 (N=number of elements along each edge) to show the convergence of the solutions for the AQR8 element. The results of the normalized displacement at the midside of the free-edge are shown in Table 6. The results for other elements are also shown in Table 6 for comparison. The mesh for this problem is comprised of rectangular shaped elements and all the elements in the table seem to perform well.

Conclusions

A 4-node quadrilateral shell element with 24 degrees of freedom has been developed which alleviates most of the deficiencies associated with 4-node shell elements. The element is based on the assumed-stress hybrid/mixed formulation using the Hellinger-Reissner principle. The membrane part of this element has 12 degrees of freedom and includes the drilling (in-plane rotational) degrees of freedom at the nodes. The bending part of this element also has 12 degrees of freedom. The bending part is of class C^0 and takes into account the transverse shear deformations. Both in-plane and out-of-plane displacements are assumed to have quadratic variations along the edges of the element, while both in-plane and out-of-plane rotations are assumed to vary linearly. A 9-parameter stress field is assumed for the membrane part and a 13-parameter stress field is assumed for the bending part. The element formulation is derived from an 8-node isoparametric element by eliminating the

midside degrees of freedom in favor of rotational degrees of freedom at corner nodes. Although the concepts of the present element are simple, the derivation and implementation of the element is somewhat awkward and indirect. Nearly all element matrices are derived based on an "internal" 8-node element.

Results from the numerical studies demonstrate that this element is accurate, passes both the membrane and the bending patch tests, does not "lock", has no spurious modes, and is nearly insensitive to mesh distortion. The present element also has the desirable property of being invariant with respect to node numbering. The results indicate that whereas the present element offers little advantage for problems with nearly rectangular meshes, it produces more accurate results when dealing with distorted meshes, than the other elements for the majority of test cases in this paper. This is important in general modeling of shell problems and adaptive refinement. The results also indicate that the present element produces more accurate results than the other elements in this paper when dealing with nearly incompressible materials, which is a consequence of assumed-stress hybrid element formulation.

Results obtained to date warrant further research in making the element formulation more direct and extending the capabilities of the element to include stability analysis, dynamic analysis, and non-linear analysis.

References

1. Irons, B. M.; and Ahmad, S.: Techniques of Finite Elements. John Wiley and Sons, New York, 1980.

2. Allman, D. J.: A Compatible Triangular Element Including Vertex Rotations for Plane Elasticity Analysis. Computers and Structures, Vol. 19, No. 1-2, 1984, pp. 1-8.

3. Cook, R. D.: On the Allman Triangle and a Related Quadrilateral Element. Computers and Structures, Vol. 22, No. 6, 1986, pp. 1065-1067.

4. MacNeal, R. H.; and Harder R. L.: A Refined Four-Noded Membrane Element with Rotational Degrees of Freedom. Computers and Structures, Vol. 28, No. 1, 1988, pp. 75-84.

5. Yunus, S. H.; Saigal S.; and Cook, R. D.: On Improved Hybrid Finite Elements with Rotational Degrees of Freedom. International Journal for Numerical Methods in Engineering, Vol. 28, 1989, pp. 785-800.

6. Friedrichs, K. O.; and Dressler, R. F.: A Boundary-Layer Theory for Elastic Plates. Communications on Pure and Applied Mathematics, Vol. 14, 1961, pp. 1-33.

7. Reiss, E. L.; and Locke, S.: On the Theory of Plane Stress. Quarterly of Applied Mathematics, Vol. 19, No. 3, 1961, pp. 195-203.

8. Laws, N.: A Boundary-Layer Theory for Plates with Initial Stress. Cambridge Philosophical Society Proceedings, Vol. 62, 1966, pp. 313-327.

9. Kang, D.: Hybrid Stress Finite Element Method. Ph.D. Dissertation, Massachusetts Institute of Technology, Cambridge, MA, May 1986.

10. Pian, T. H. H.: Derivation of Element Stiffness Matrices by Assumed Stress Distributions. AIAA Journal, Vol. 2, 1964, pp. 1333-1336.

11. Pian, T. H. H.: Evolution of Assumed Stress Hybrid Finite Element. Accuracy, Reliability and Training in FEM Technology, Proceedings of the Fourth World Congress and Exhibition on Finite Element Methods, The Congress Center, Interlaken, Switzerland, Edited by John Robinson, September 17-21, 1984, pp. 602-619.

12. Pian, T. H. H.; and Sumihara K.: Rational Approach for Assumed Stress Finite Elements. International Journal for Numerical Methods in Engineering, Vol. 20, 1984, pp. 1685-1695.

13. Pian, T. H. H.: Finite Elements Based on Consistently Assumed Stresses and Displacement. Finite Elements in Analysis and Design, Vol. 1, 1985, pp. 131-140.

14. Pian, T. H. H.; and Chen, D.: On the Suppression of Zero Energy Deformation Modes. International Journal for Numerical Methods in Engineering, Vol. 19, 1983, pp. 1741-1752.

15. Robinson, J.: An Accurate and Economical Eight-Node Stress Membrane Element. International Journal for Numerical Methods in Engineering, Vol. 15, 1980, pp. 779-789.

16. Robinson, J.: Four-Node Quadrilateral Stress Membrane Element with Rotational Stiffness. International Journal for Numerical Methods in Engineering, Vol. 16, 1980, pp. 1567-1569.

17. Reissner, E.: On Bending of Elastic Plates. Quarterly of Applied Mathematics, Vol. 5, 1947, pp. 55-68.

18. Knight, N. F., Jr.; Gillian, R. E.; McCleary, S. L.; Lotts, C. G.; Poole, E. L.; Overman, A. L.; and Macy, S. C.: CSM Testbed Development and Large-Scale Structural Applications. NASA TM-4072, April 1989.

19. Stanley, G. M.; and Nour-Omid, S.: The Computational Structural Mechanics Testbed Generic Structural-Element Processor Manual. NASA CR-181728, March 1990.

20. MacNeal, R. H.; and Harder, R. L.: A Proposed Standard Set of Problems to Test Finite Element Accuracy. Finite Elements in Analysis and Design, Vol. 1, No. 1, 1985, pp. 3-20.

21. Timoshenko, S. P.; and Goodier, J. N.: Theory of Elasticity, McGraw-Hill, Third Edition, 1970.

22. Scordelis, A. C.; and Lo, K. S.: Computer Analysis of Cylindrical Shells. Journal of the American Concrete Institute, Vol. 61, 1969, pp. 539-561.

23. MacNeal, R. H.: A Simple Quadrilateral Shell Element. Computers and Structures, Vol. 8, 1978, pp. 175-183.

24. Park, K. C.; and Stanley, G. M.: A Curved C^0 shell Element Based on Assumed Natural-Coordinate Strains. Journal of Applied Mechanics, Vol. 108, 1986, pp. 278-290.

25. Stanley, G. M.: Continuum-Based Shell Elements. Ph.D. Dissertation, Stanford University, Stanford, CA, August 1985.

26. Rankin, C. C.; Stehlin, P.; and Brogan, F. A.: Enhancements to the STAGS Computer Code. NASA CR-4000, 1986.

27. Aminpour, M. A.: Assessment of SPAR Elements and Formulation of Some Basic 2-D and 3-D Elements for Use with Testbed Generic Element Processor. Proceedings of NASA Workshop on Computational Structural Mechanics - 1987, NASA CP-10012-Part 2, Nancy P. Sykes, (Editor), 1989, pp. 653-682.

Appendix

The following is a brief description of the elements used in Tables 1-6 for comparison with the element developed in this paper.

The QUAD4 MSC/NASTRAN element is a 4-node isoparametric shell element with selective reduced-order integration. The transverse shear uses a string-net approximation and augmented shear flexibility[23]. This element was developed by MacNeal and is available in the MSC/NASTRAN finite element code.

The Q4S element is a 4-node shell element in which the membrane part is formulated internally as an 8-node isoparametric element with selective reduced-order integration and later reduced to a 4-node element by eliminating the midside degrees of freedom in favor of rotational degrees of freedom at the corner nodes. This element was developed by MacNEAL[4]. The bending part of the Q4S is the same as that of the QUAD4[4].

The AQ element is a 4-node assumed-stress hybrid/mixed membrane element which is formulated internally as an 8-node isoparametric membrane element and later reduced to a 4-node membrane element by eliminating the midside degrees of freedom in favor of rotational degrees of freedom at the corner nodes. This element was developed by Yunus et al.[5]. The only result reported in reference [5] for the cantilever beam problem in Table 1 using the AQ element is for the mesh with trapezoidal-shaped elements with a unit in-plane end moment. This result is reported to be .85. The difference in the results between the AQ membrane element and the membrane part of AQR8 is in the selection of the assumed-stress functions.

The ES1/EX47 element is a 4-node C^0 isoparametric assumed natural-coordinate strain (ANS) shell element developed by Park and Stanley[24-25] and implemented in the CSM Testbed Software System[18] by Stanley using the generic element processor template[19]. This element is not invariant and does not pass the patch test. This element does not include the drilling degrees of freedom in the formulation.

The ES5/E410 element is a 4-node C^1 shell element which was originally implemented in the STAGS finite element code and later in the CSM Testbed by Rankin[26]. This element includes the rotational degrees of freedom in its formulation and uses cubic interpolation for all displacement fields. This element is not invariant and does not pass the patch test.

The ES4/EX43 element is a simple 4-node C^0 isoparametric assumed-stress hybrid/mixed shell element implemented in the CSM Testbed by this author[27]. This element passes the patch test and is invariant with respect to node numbering. This element does not include the drilling degrees of freedom in its formulation and uses linear interpolation for all displacement and rotation fields.

16

Table 1. Normalized tip displacements in direction of loads for straight cantilever beam.

Tip Loading Direction	QUAD4 MSC/ NASTRAN	ES1/ EX47[†]	ES5/ E410[†]	ES4/ EX43	AQR8 (present)
(a) rectangular shaped elements					
Extension	.995	.995	.994	.996	.998
In-plane Shear	.904*	.904	.915	.993	.993
Out-of-Plane Shear	.986	.980	.986	.981	.981
Twist	.941**	.856	.680	1.023	1.011
End Moment	—	.910	.914	1.000	1.000
(b) trapezoidal shaped elements					
Extension	.996	.761	.991	.999	.998
In-plane Shear	.071*	.305	.813	.052	.986
Out-of-Plane Shear	.968	.763	#	.075	.965
Twist	.951**	.843	#	1.034	1.029
End Moment	—	.505	.822	.102	.996
(c) parallelogram shaped elements					
Extension	.996	.966	.989	.999	.998
In-plane Shear	.080*	.324	.794	.632	.977
Out-of-Plane Shear	.977	.939	.991	.634	.980
Twist	.945**	.798	.677	1.166	1.159
End Moment	—	.315	.806	.781	.989

† These elements are not invariant and do not pass the patch test.

* The results from MacNeal's Q4S element for in-plane shear load are reported in reference [4] to be .993, .988, and .986 for the meshes in (a), (b), and (c) respectively.

** These results for twist were normalized with .03028 in reference [20]. Herein, all the other results for twist are normalized using .03046 according to Timoshenko and Goodier's Theory of Elasticity[21].

\# The element produces a singular stiffness matrix for this mesh.

Table 2. Normalized tip displacements in direction of loads for curved cantilever beam.

Tip Loading Direction	QUAD4 MSC/ NASTRAN	ES1/ EX47	ES5/ E410	ES4/ EX43	AQR8 (present)
In-plane Shear	.833	.929	.938	.888	.997
Out-of-Plane Shear	.951	.935	.887	.925	.956

Table 3. Normalized tip displacements in direction of loads for twisted cantilever beam.

Tip Loading Direction	QUAD4 MSC/ NASTRAN	ES1/ EX47	ES5/ E410	ES4/ EX43	AQR8 (present)
In-plane Shear	.993	1.357	1.054	1.361	.991
Out-of-Plane Shear	.985	1.293	1.173	1.359	1.093

Table 4. Normalized vertical deflection at point C for tapered and swept panel.

Mesh	AQ	ES1/ EX47	ES5/ E410	ES4/ EX43	AQR8 (present)
2×2	.914	.880	.873	.882	.930
4×4	.973	.953	.953	.962	.979

Table 5. Normalized radial displacements at inner boundary for thick-walled cylinder.

Poisson's Ratio	QUAD4 MSC/ NASTRAN	ES1/ EX47	ES5/ E410	ES4/ EX43	AQR8 (present)
0.49	.846	.831	.848	.990	.989
0.499	.359	.352	.360	.990	.988
0.4999	.053	.052	.053	.990	.988

Table 6. Normalized displacements at the midpoint of the free-edge for Scordelis-Lo roof.

Mesh	QUAD4 MSC/ NASTRAN	ES1/ EX47	ES5/ E410	ES4/ EX43	AQR8 (present)
2×2	1.376	1.387	1.384	1.459	1.218
4×4	1.050	1.039	1.049	1.068	1.021
6×6	1.018	1.011	1.015	1.028	1.006
8×8	1.008	1.005	1.005	1.017	1.003
10×10	1.004	1.003	1.001	1.011	1.001
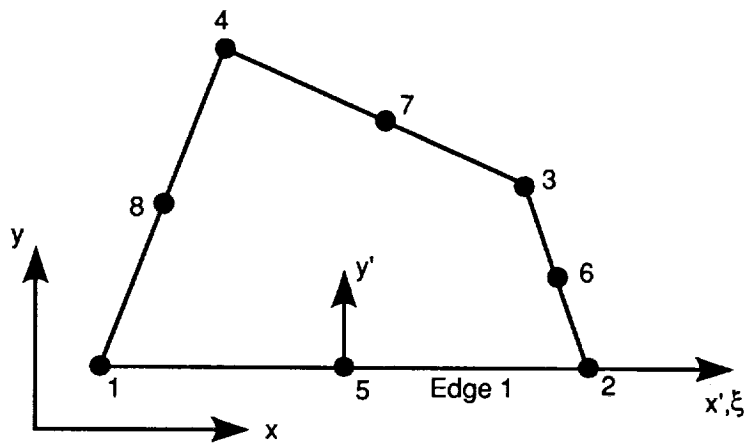
Figure 1.   Element coordinate system definition.
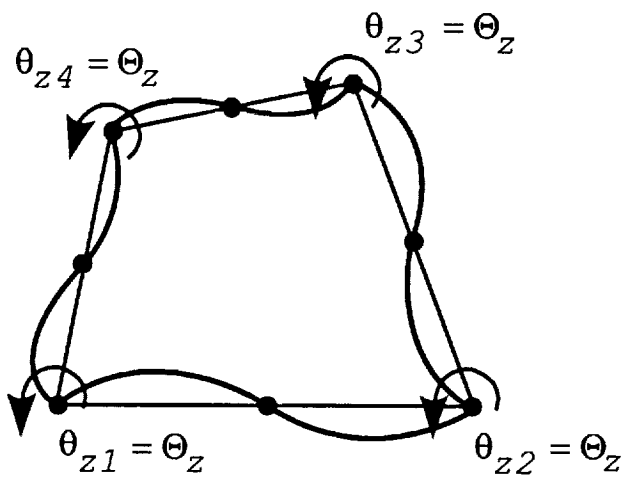
Figure 2.   The "zero displacement" mode.
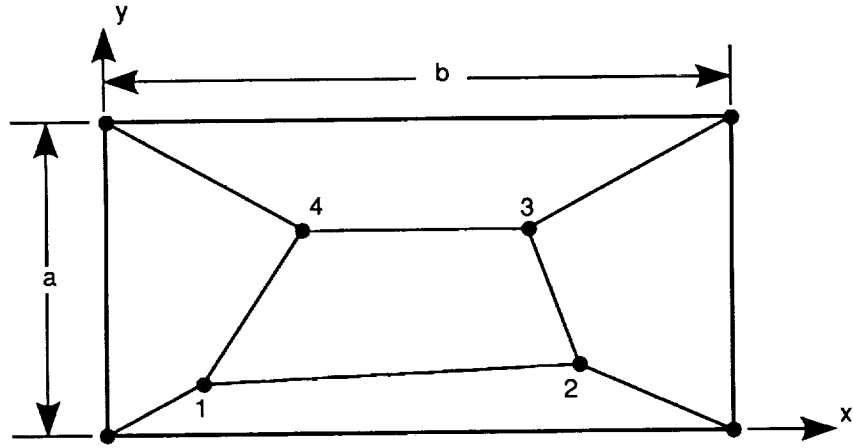
Location of nodes:

node	x	y
1	.04	.02
2	.18	.03
3	.16	.08
4	.08	.08

Applied displacements:

(a) Membrane patch test

Boundary conditions: $u = 10^{-3}(x + y/2)$
$v = 10^{-3}(x/2 + y)$

Theoretical solution: $\epsilon_{xx} = \epsilon_{yy} = \gamma_{xy} = 10^{-3}$
$\sigma_{xx} = \sigma_{yy} = 1333., \sigma_{xy} = 400.$

(b) Bending patch test

Boundary conditions: $w = -10^{-3}(x^2 + xy + y^2)/2$
$\theta_x = -10^{-3}(x/2 + y)$
$\theta_y = -10^{-3}(x + y/2)$

Theoretical solution:

Bending moments per unit length:
$M_x = M_y = 1.111 \times 10^{-7}, M_{xy} = 3.333 \times 10^{-8}$

Surface stresses:
$\sigma_{xx} = \sigma_{yy} = \pm 0.667, \sigma_{xy} = \pm 0.200$

Figure 3. The patch test problem. a=0.24, b=0.12, t=0.001, E=10^6, ν=0.25.
(Consistent units are used for various properties.)

a) rectangular shape elements

b) trapezoidal shape elements

c) parallelogram shape elements
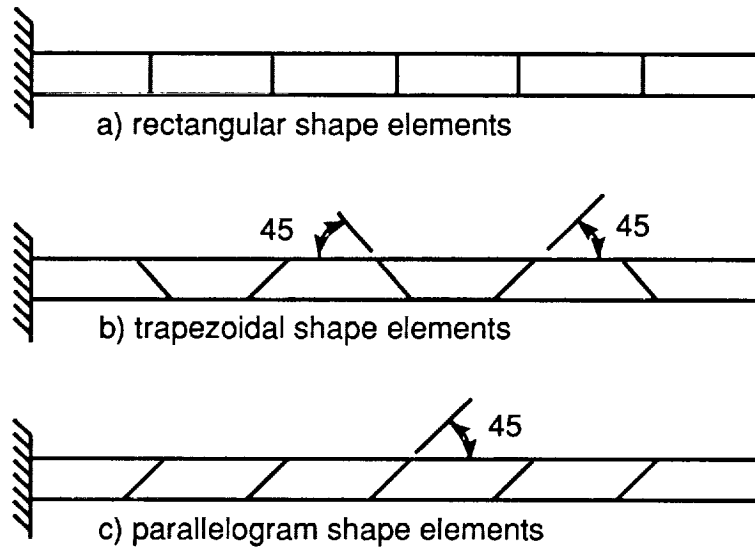
Theoretical solutions:

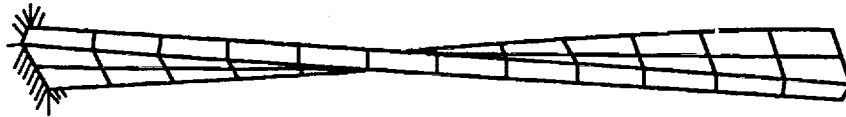| Tip load direction	Displacement in direction of load
Extension	$.3 \times 10^{-4}$
In-plane shear	.1081
Out-of-plane shear	.4321
Twist	.03406
In-plane moment	.009

Figure 4. Straight cantilever beam problem. Length=6., height=0.2, depth=0.1, E=10^7, ν=0.3, mesh=6×1. Loading: unit forces at the free end.
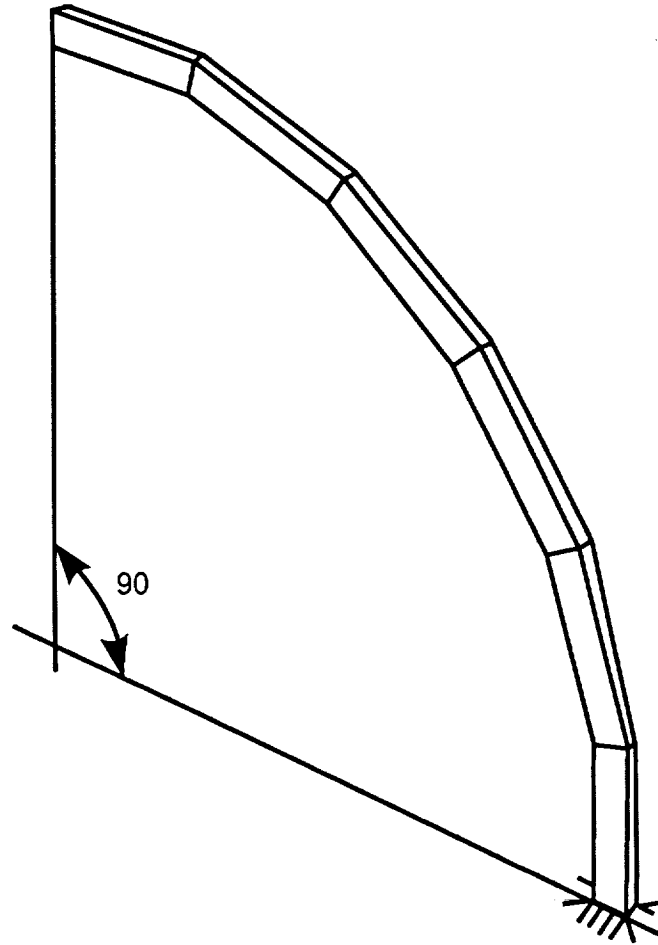
90

Theoretical solutions:

Tip load direction	Displacement in direction of load
In-plane shear	.08734
Out-of-plane shear	.5022

Figure 5. The curved cantilever beam problem. Inner radius=4.12, outer radius=4.32, depth=0.1, E=10^7, ν=0.25, mesh=6×1. Loading: unit forces at the free end. (Consistent units are used for various properties.)

Theoretical solutions:

Tip load direction	Displacement in direction of load
In-plane shear	.005424
Out-of-plane shear	.001754

Figure 6. The twisted cantilever beam problem. Length=12., width=1.1, depth=0.32, twist=90⁰ (root to tip), E=29.×10^6, ν=0.22, mesh=12×2. Loading: unit forces at the free end.
(Consistent units are used for various properties.)

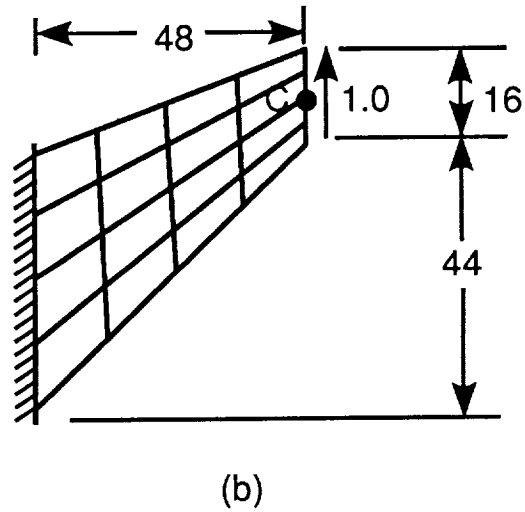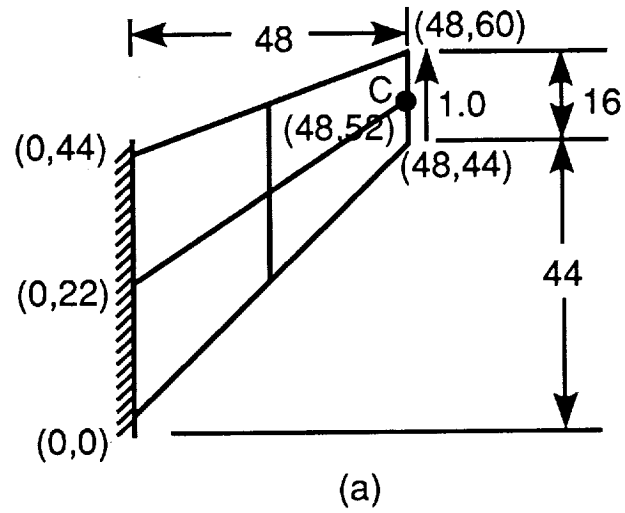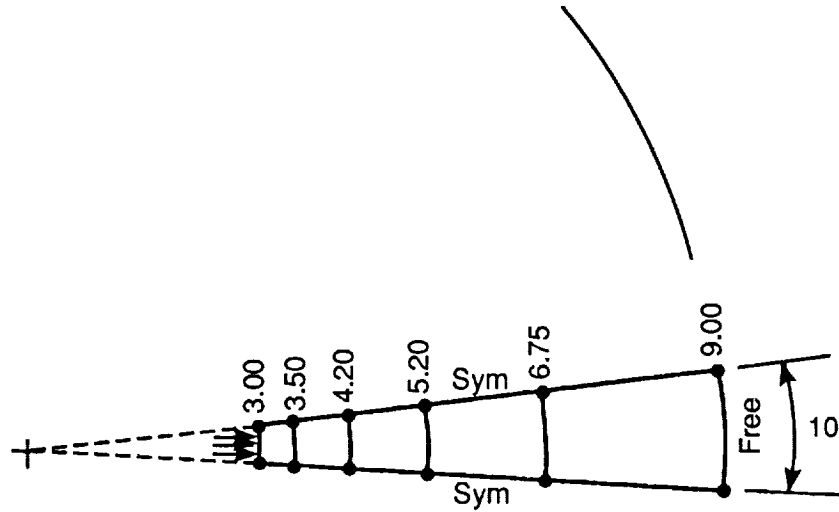Figure 7. The tapered and swept panel problem. Thickness=1., E=1., ν=1/3, mesh=N×N. Loading: unit in-plane shear force distributed on the free edge. Reference solution: vertical displacement at C=23.90 from reference [10]. (a) 2×2 mesh, (b) 4×4 mesh. (Consistent units are used for various properties.)

25

Theoretical solutions:

$$u(r) = \frac{(1+\nu)pR_1^2}{E(R_2^2 - R_1^2)}[R_2^2/r + (1-2\nu)r]$$

where p=pressure on the inner surface, R_1=inner radius, R_2=outer radius.

Poisson's ratio, ν	Radial displacement at $r = R_1$
.49	5.0399×10^{-3}
.499	5.0602×10^{-3}
.4999	5.0623×10^{-3}

Figure 8. The thick-walled cylinder problem. Inner radius=3., outer radius=9., thickness=1., E=1000., plane strain condition, mesh=5×1 as shown. Loading: unit pressure on inner boundary.
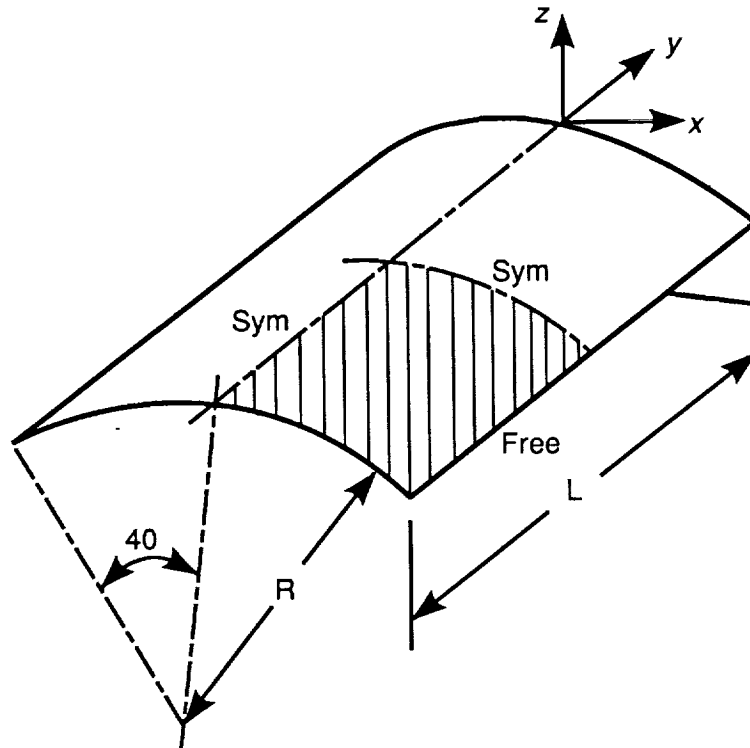(Consistent units are used for various properties.)

Figure 9. The Scordelis-Lo roof problem. Length=50., radius=25., thickness=0.25, $E=4.32\times10^{8}$, $\nu=0.3$, mesh=N×N. Loading: 90. per unit area in vertical direction, i.e., gravity load; $u_x=u_z=0$ on curved edges. Reference solution: vertical displacement at midpoint of free-edge=0.3024 from reference [23]. (Consistent units are used for various properties.)

Report Documentation Page

1. Report No. NASA CR-4279	2. Government Accession No.	3. Recipient's Catalog No.
4. Title and Subtitle A 4-Node Assumed-Stress Hybrid Shell Element With Rotational Degrees of Freedom		5. Report Date April 1990
		6. Performing Organization Code
7. Author(s) Mohammad A. Aminpour		8. Performing Organization Report No.
9. Performing Organization Name and Address Analytical Services and Materials, Inc. Hampton, VA 23666		10. Work Unit No. 505-63-01-10
		11. Contract or Grant No. NAS1-18599
12. Sponsoring Agency Name and Address National Aeronautics and Space Administration Langley Research Center Hampton, VA 23665-5225		13. Type of Report and Period Covered Contractor Report
		14. Sponsoring Agency Code

15. Supplementary Notes
Langley Technical Monitor: W. Jefferson Stroud

16. Abstract

An assumed-stress hybrid/mixed 4-node quadrilateral shell element is introduced that alleviates most of the deficiencies associated with such elements. The formulation of the element is based on the assumed-stress hybrid/mixed method using the Hellinger-Reissner variational principle. The membrane part of the element has 12 degrees of freedom including rotational or "drilling" degrees of freedom at the nodes. The bending part of the element also has 12 degrees of freedom. The bending part of the element uses the Reissner-Mindlin plate theory which takes into account the transverse shear contributions. The element formulation is derived from an 8-node isoparametric element. This process is accomplished by assuming quadratic variations for both in-plane and out-of-plane displacement fields and linear variations for both in-plane and out-of-plane rotation fields along the edges of the element. In addition, the degrees of freedom at midside nodes are approximated in terms of the degrees of freedom at corner nodes. During this process the rotational degrees of freedom at the corner nodes enter into the formulation of the element. The stress field is expressed in the element natural-coordinate system such that the element remains invariant with respect to node numbering. The membrane part of the element is based on a 9-parameter stress field, while the bending part of the element is based on a 13-parameter stress field. The element passes the patch test, is nearly insensitive to mesh distortion, does not "lock", possesses the desirable invariance properties, has no spurious modes, and for the majority of test cases used in this paper produces more accurate results than the other elements employed herein for comparison.

17. Key Words (Suggested by Authors(s)) assumed-stress, hybrid, mixed, element, finite element, quadrilateral, shell, drilling, variational	18. Distribution Statement Unclassified—Unlimited
	Subject Category 39

19. Security Classif.(of this report) Unclassified	20. Security Classif.(of this page) Unclassified	21. No. of Pages 28	22. Price A03